A Floor Power Module for Cooperative 3D Printing

Jacob Currence, Rolando Morales-Ortega, Jason Steck, Wenchao Zhou

The AM³ Lab, Department of Mechanical Engineering, University of Arkansas at Fayetteville
Fayetteville, AR, United States of America; Corresponding email: zhouw@uark.edu

Abstract

Cooperative 3D printing is an emerging technology that utilizes multiple printhead-carrying mobile robots to work simultaneously to 3D print or assemble products on a factory floor, which can provide the scalability, increased printing capability, and reduced human intervention for 3D printing to potentially become a mainstream digital manufacturing technology. However, powering the mobile printers for them to span entire factory floors poses an issue. Traditional cords are not an option due to restricting free movement across long distances. On-board batteries would waste energy due to additional weight and the need to recharge could interrupt ongoing print jobs and increase printing time. In this paper, we present an electrified floor to power the mobile printers wirelessly. First, we designed a floor module with stainless steel conductive strips in a concrete base and a brush that is carried by the mobile robots to make sure it never loses contact with the electrified floor while in motion. Then we designed a circuit to sort the polarity of the current from the floor based on the power requirements of the robot. A prototype of the floor power module was then developed and tested with a mobile 3D printer. Results show the developed floor power supply can power the mobile 3D printers effectively. This development will potentially enable an autonomous factory equipped with thousands of mobile 3D printers powered wireless by the factory floor.

Keywords: Additive manufacturing; cooperative 3D printing; power system; mobile robot

1. Introduction

3D printing has quickly grown from a rapid prototyping tool to a serious contender of digital manufacturing over the past three decades [1-4]. Several major issues are still plaguing this technology for it to become a mainstream digital manufacturing method, including the limit in maximum print size, long printing time, printing complex products, and printing quality [5, 6]. Cooperative 3D printing is an emerging 3D printing technology that employs a plurality of mobile robots carrying different printheads to 3D print and assemble products on a factory floor. By freeing the printhead out of a "box", the mobile 3D printers will be able to print over the entirety of factory floors and cooperate with each other to provide the scalability in both print size and print time while also enhancing the printing capability and quality by carrying different types of "printheads" (e.g., a gripper for incorporating pre-manufactured components, an inkjet printhead for high resolution printing, etc.). However, powering these mobile robots wirelessly poses an issue for this technology.

The power source of a mobile robot is often the limiting factor for its maximum operating time without interruption, as well as its ultimate maneuverability and effective working space. Within the manufacturing industry, there has been significant work done in developing power sources for mobile robots, ranging from rechargeable/replaceable batteries [7-10], hybrid fossil

fuel-electric motors [11-13], and various solar, fuel cell, and hydraulic-electric power systems [14-19]. Batteries are by far the most common form of mobile power storage, which can be a valid candidate for powering a mobile 3D printer. Battery-powered systems are highly mobile, and it is essential that a 3D printer is operated indoors, which makes it difficult to use solar or combustion-electric power sources. However, batteries are heavy to carry and must be accompanied by an additional power source or charging station if they are to operate for long periods of time on a single charge. Solutions include the onboard AC generator on the AURORA agricultural robot [20], charging stations utilized by KIVA Systems factory robots [21], and a tethered power cable such as in the HYPOS tethered power supply [8]. The fundamental requirement of a mobile 3D printing power source is that operation is not interrupted during the printing process, in particular for a print with numerous cooperative mobile 3D printers. In addition, any wired power source poses issues with cord tension disturbing the delicate printing process or blocking the paths of the mobile robots. Therefore, all aforementioned solutions are eliminated for application to the mobile robots for cooperative 3D printing, and there exists a distinct need for a novel wireless power source for indoor mobile robots requiring long-term uninterrupted operation.

In this paper, we present an electrified floor to wirelessly power mobile 3D printers, which allows for a constant wireless power source operating independent of any wires or energy storage devices. This design draws inspiration from the design of bumper car power systems where each bumper car draws power through a direct connection with a powered floor [22]. The bumper car power system occasionally loses power and relies significantly on the momentum of the bumper car to restore connection with the power floor, while the mobile 3D printer must never lose power during the printing. Besides, the scale of the geometry and power requirement is very different from what is needed for a mobile 3D printer, which calls for a different design. In this paper, we present a power floor to meet the requirements of cooperative 3D printing. First, we design a power floor with electrified stainless steel conductive strips of alternating polarity installed within a concrete base. A brush apparatus is then designed to be carried by the robots across the conductive strips, transferring power from the floor to the robot while in motion. A rectifier circuit is then designed to sort the polarity of the current from the floor based on the power requirements of the robot, such that current flows in the correct direction regardless of the polarity of the active strips. A prototype of the floor power module is then developed and tested with a mobile 3D printer. Results show the developed floor power module can power the mobile 3D printers effectively. This development will potentially enable an autonomous factory equipped with thousands of mobile 3D printers powered wirelessly by the factory floor.

This paper is organized as follows. In section 2, the engineering requirements and design of a floor power module, brush apparatus, and rectifier circuit compatible with an existing mobile 3D printer are presented. Section 3 presents the prototyping process of the designs. Then testing and results are discussed in section 4. Conclusions are given in section 5

2. Design

Recently, a mobile robot equipped with a Fused Deposition Modeling (FDM) printhead has been developed in the AM^3 Lab at the University of Arkansas for cooperative 3D printing, as

shown in Figure 1, which envisions an autonomous factory equipped with many of these mobile robots that work cooperatively to print and assembly products.

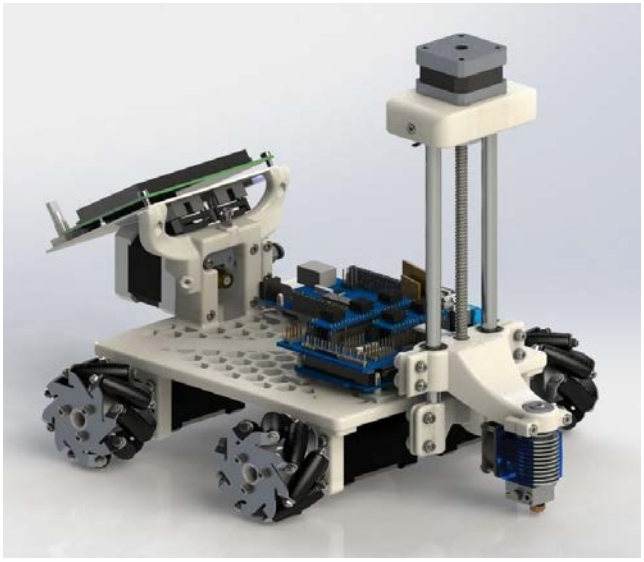

Figure 1. Mobile 3D printer design.

Our objective is to design a power module that provides wireless, uninterrupted power to multiple mobile 3D printers for use in cooperative 3D printing, such that no onboard power sources are required (e.g., batteries). A design inspired by the bumper car powering system has been pursued. The floor surface on which the robots move and print consists of parallel conductive metal strips that are each separated by an insulator. These conducting strips alternate positive and negative charge, one after another. A brush apparatus is then designed which transfers power from the floor to the mobile 3D printer by making contact with at least one positive and negative strip at any time while mounted to the robot. To then sort the incoming polarity, a rectifier circuit is needed to ensure the current flows in the desired direction no matter the polarity of each brush. In this paper, the three components of the floor power module (i.e., floor surface, brush apparatus, and rectifier circuit) are each designed in sequence, and a schematic of the resulting system is shown in Figure 2:

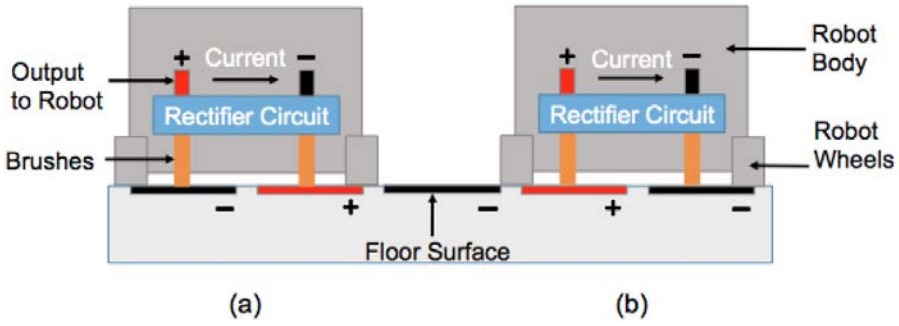

Figure 2. Cross-sectional view of the floor power module and each component, where the polarity of the strips in contact changes while the direction of current delivered to the robot remains the same.

2.1 Floor Surface Design

2.1.1 Design Constraints

A series of engineering requirements were developed for the floor surface that would successfully provide power to a mobile 3D printer:

1. Conductivity: The conductive strips must have a low resistance to current. This is important due to the potentially large areas of floor transmitting power, thus making the resistance of each strip a main factor of the power module's efficiency. Therefore, it is set that the floor must be able transmit 12 volts and 10 amps of power over distances greater than 5 ft with a voltage drop less than 2 V for our prototype design.
2. Insulating strips: To couple with the conductive strip material, an insulating material must be chosen so that it completely insulates the conductive strips from one another. These are necessary to having adjacent conductive strips of opposite polarity.
3. Durability: The floor must be able to withstand the electric and mechanical stresses put upon it by the robots brushes and wheels, and it must be able to withstand years of wear with little to no maintenance. This applies to both conductive and insulating strips. In case of damage, it must be easy to repair or replace at low cost.
4. Short circuit prevention: To prevent short circuiting between the floors strips and the robots brushes, the insulating layer in between the strips must be uniform and wider than the diameter of a single brush. That is, a brush above the insulating layer must not touch both conductive strips (which would cause a short circuit).
5. Manufacturability: The materials must be practical at both the small and large scales, inexpensive, and easy to manufacture. The total cost of the floor should be kept under $\$10/ft^2$.
6. Safety: the electrified floor must operate within safety limits for humans to walk on.
7. Traction: The floor must have a sufficient high friction coefficient to provide enough traction for the wheels of the robot such that it doesn't slip.

2.1.2 Conductive Strip Material Selection

After researching commercially available materials that are both conductive and strong, it was decided to use brushed 304 stainless steel, which has a conductivity of 2.39% of international annealed copper standard (IACS) [23]. To carry the needed voltage and current, we need to determine the resistance of the conductive strip, which can be calculated according to Equation 1, where R is the resistance, ρ is the resistivity of the material, L is the length of the strip, and A is the cross-sectional area of the strip:

$$R = \rho L/A \tag{1}$$

These dimensions must be balanced with the cost of material, while remaining compatible with the overall geometry of the floor and brushes. It was initially assumed that the width of the strips must be 1.5 in. Given the resistivity of 304 stainless steel is 7.2E-7 ohm-m [23] and the desired strip length of 5 ft, the thickness of each strip was calculated to be 0.018 inches thick when rounded to fit within the range of pre-manufactured 304 stainless steel sheets. In the future, these floors may be the size of entire factories, spanning hundreds of feet. The strips must be able to

carry the power long distances without losing much of its initial power. Given the dimensions of the strips and the power requirements, the voltage drop across each strip may be calculated using Ohm's Law in Equation 2:

$$V_{drop} = IR \tag{2}$$

In regard to surface durability, 304 Stainless steel is very strong and corrosion resistant. With a hardness of B82 on the Rockwell B scale [24], it will not be easily worn by the sliding brushes. Moreover, its corrosion resistant properties will keep it free from rust and allow for easy cleaning. This alleviates concerns of the sliding brushes damaging the floor surface during operation.

2.1.3 Insulating Strip Material Selection

A marine grade epoxy was then used for the insulating strips, as well as for the binding material between the steel strips and the concrete base. This material was chosen for its ease of manufacturing and replacement, along with sufficient durability and insulating properties. The epoxy allows for a liquid to be poured into the void space between the steel strips, and after hardening they can be sanded flat, creating a seamless transition between strips. This installation process is described further in section 3 of this paper. Similar to stainless steel, marine epoxy is also corrosion resistant. Although the epoxy is softer than both the stainless-steel strips and the chosen brush material, it will still have a relatively long effective life due to low pressure and friction of the brushes upon it, and it is the cheapest and easiest to repair or replace out of all materials used in the floor power module.

2.1.4 Cost Analysis

The floor materials chosen are both relatively cheap and easy to obtain. 304 brushed stainless steel sheets can be purchased in bulk for approximately $2 per cubic inch. This price drops significantly as bulk of purchase goes up. With the chosen thickness of 0.018 in, the stainless steel strips will cost about $5 per square foot of floor for small scale builds. The marine epoxy comes in at approximately $0.34 per cubic inch. For the design application of 0.018 inches plus the sanded excess, the cost of the epoxy is approximately $0.05/ft^2. In the case of a 2500 square foot factory, the cost of materials to install our design of powered floor would cost less than $7500 as shown in Table 1.

Table 1. Approximate relative costs of different floor sizes.

	Stainless Steel Cost	Epoxy Cost	Full Floor Cost
Small to medium scale floor (4 ft^2)	$5/ft^2	$0.05/ft^2	$20.20
Large scale floor (2500 ft^2)	$2.85/ft^2	$0.05/ft^2	$7250

With the chosen thickness of 0.018 in, the stainless-steel sheets can be cut easily using common machinery. On a larger scale, the strips may need to be pre-cut by the manufacturer. The

epoxy can be sanded down using industrial sanders on a small and large scale at relatively low cost. Therefore, it is possible to keep the total cost of the floor under $\$10/ft^2$.

2.2 Brush Apparatus

2.2.1 Design Constraints

The brush apparatus is carried by the mobile robot to draw power from the electrified floor. In a similar fashion to the design of the floor surface, a series of engineering requirements were taken into consideration during the design:

1. Geometry: The brushes must be arranged in a geometric pattern that ensures at least one brush is in connection with a positive strip and another in connection with a negative strip. This must be the case at all times no matter the location or orientation of the robot on the floor. In addition, a single brush must not touch both a positive and negative strip simultaneously, as this would cause a short circuit.
2. Reliability: The brushes must keep constant contact with the floor in order to ensure constant power, including when the brushes encounter defects or debris. In particular, the brushes must not have issues crossing between each adjacent strip. For example, the brush must not get caught on the insulating layer as it slides across the surface.
3. Dimensions: The brushes must be mounted underneath the robot in order to reach the floor. This leaves open only one spot to mount the brushes with the current mobile 3D printer design: a small central area under the robot between the stepper motors as can be seen in Figure 1. This equates to a rectangular prism 6x3.5 inch wide and 2.1 inch tall.
4. Brush material: The material used for the brushes must be conductive, mechanically resilient (strength and hardness), and economically viable (low cost and ease of manufacturability). To prevent excessive scratching of the floor surface, the brush material must have a Rockwell hardness value within 5 of the chosen floor material.

2.2.2 Brush Geometry

The mobile 3D printer will carry a set of brushes along the floor power module that allows the robot to switch between conductive strips without disconnecting from power. In order to provide continuous power, there must be at least one brush on each polarity of strip at all times. The more brushes in contact with the strips on the floor the more chances there are that one of them will lay on a positive strip and other one on a negative strip. However, since having an excess of brushes can be both expensive and impractical, it was imperative to reduce the number of brushes by strategically selecting their positions. The positioning of the brushes relative to each other is defined as the geometric configuration. A feasible geometric configuration for the brushes will be determined below.

2.2.2.1 Two Brushes

Geometric analysis begins by establishing the constraint that at least two brushes are required at all times, one for positive and one for negative. If there are only two brushes on the power module, these are free to move vertically from end to end while providing continuous

power. However, horizontal displacement is restricted, since as soon as one brushes encounters an insulating strip, the circuit is disconnected. This event is illustrated in Figure 3. This indicates that two brushes are not sufficient for powering the circuit.

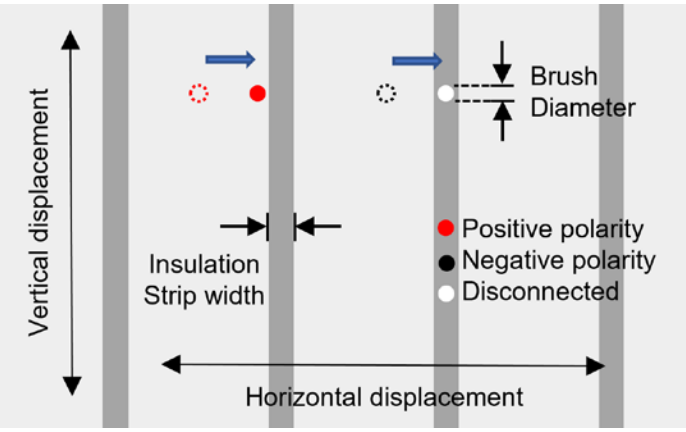

Figure 3. Illustration of two brushes at the moment of disconnection during horizontal movement. The dotted circles represent the brush locations before movement and the solid circles represent the brush locations after the movement.

2.2.2.2 Three Brushes

By then adding a third brush to the configuration, the issue with horizontal movement can be solved, as illustrated in Figure 4(a). As the brush apparatus moves across the floor surface, each brush transitions across an insulated strip without losing overall power. However, an equivalent issue arises when rotational motion is considered. It is found that as the robot transitions from horizontal to vertical, the horizontal distance covered by the brushes decreases until it is unable to cover the distance to touch at least one positive and negative strip. This issue is depicted in Figure 4(b), and suggests that the rotation of the brush geometry must place one brush on either of the farthest sides of the geometry, such that both strips are in contact.

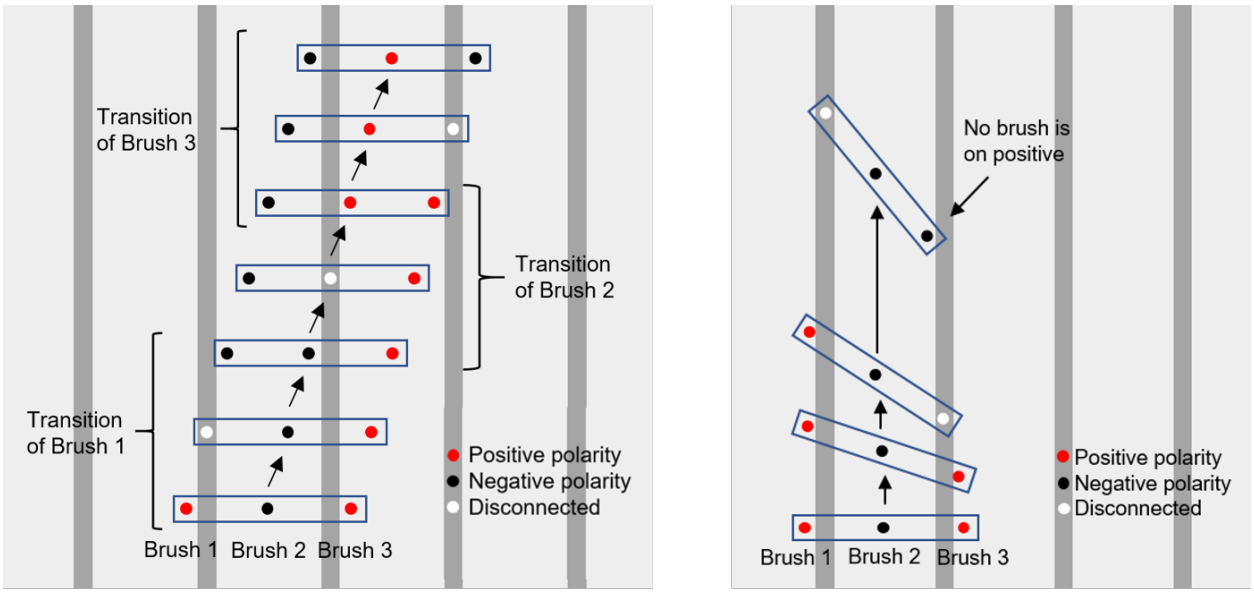

(a) (b)

Figure 4. Geometry diagram with three brushes: (a) translational motion; (b) rotational motion.

2.2.2.3 Four Brushes

From the previous arrangement, it is clear that a geometric configuration with at least four brushes is required to achieve continuous power supply when the robot is subjected to both translational and rotational displacements. By positioning three brushes in an equilateral triangle, and by placing the fourth brush at the center of a circle intersecting each vertex of the triangle, a geometric configuration for four brushes is obtained. This configuration has four critical positions, as shown in Figure 5(a). To analyze potential disconnections during translational displacements, the position of each brush is projected onto the horizontal in Figure 5(a). These horizontal positions are then translated across the floor surface in Figure 5(b). In the same fashion as Figure 4(a), each brush transitions through positive, disconnected, and negative while there is at least one brush on positive and one brush on negative, thus maintaining a complete circuit throughout the movement. However, it is still necessary to identify disconnections during rotation. By observation, no degree of angular displacement causes loss of contact with positive and negative simultaneously. For example, rotating clockwise the geometric configuration across the floor between positions 1 and 2, the rightmost brush loses contact with the positive strip while the leftmost brush is just beginning its positive motion (i.e., as one brush disconnects, the opposing brush is moving *onto* a strip instead of *away*, thus maintaining a closed circuit). This extends to every other position, since as one brush in transitioning, another is soundly connected the corresponding strip. Therefore, an equilateral triangle and central brush arrangement is determined to be a sufficient geometric configuration, and is then used for designing the brush apparatus.

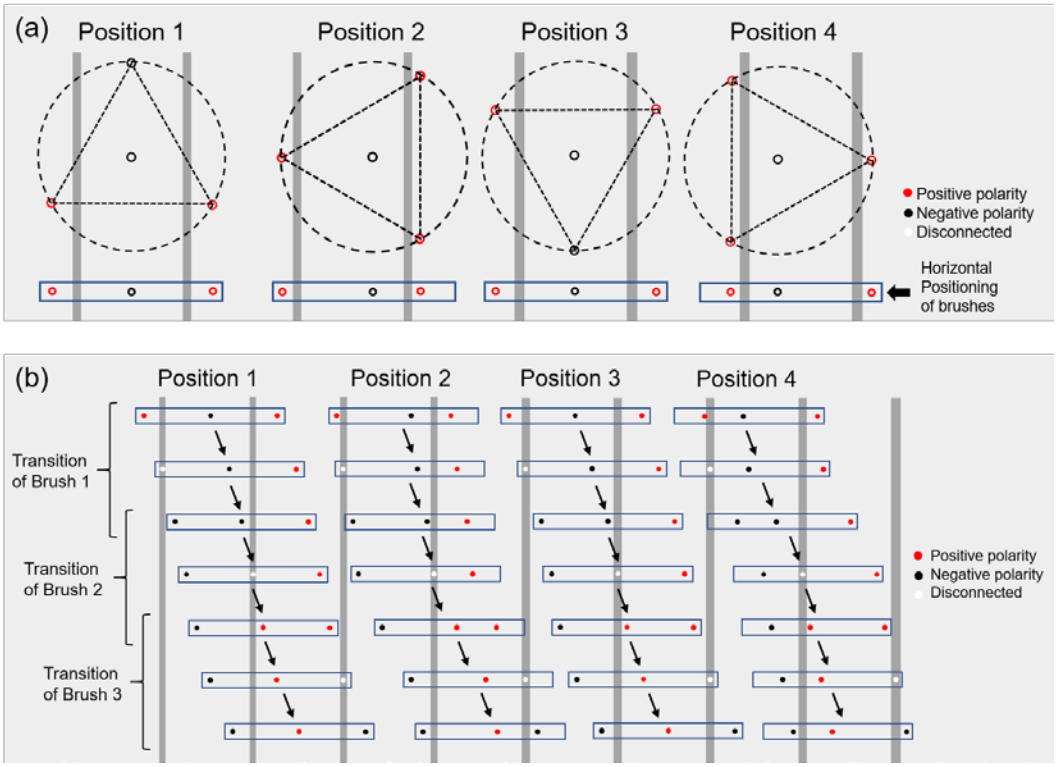

Figure 5. Four critical brush positions for equilateral triangle geometry: (a) Circular positions projected onto the horizontal plane; (b) translational motion of each configuration as each brush position transitions through positive, disconnected, and negative.

2.2.2.4 Dimensional Proportionality

After determining that the equilateral triangle is a suitable geometrical configuration, it is necessary to determine the relations between triangle size and strip width. The dimensions of the geometric configuration formed by the brushes and the width of the floor strips have a direct correlation (defined proportionalities) that make them interact with each other in a way that provides a constant transmission of electrical power from the floor to the main circuit.

First, the size of the area covered by the robot will determine the size of the geometrical configuration since the brushes will be within the perimeter covered by the robot. The size of the triangle will always be smaller in size than the area covered by the robot to protect the brushes from other objects on the power module floor and avoid loss of electrical power. The dimensions of the floor surface and brush geometry are defined in Figure 6:

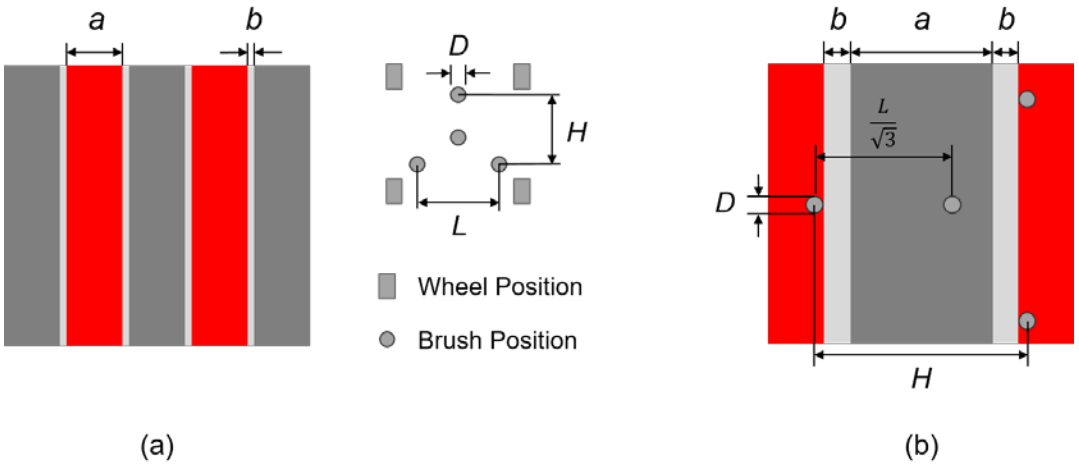

Figure 6. (a) Dimensions of the floor surface and brushes; (b) brush geometry on floor surface in position 2 of Figure 5(a).

The relations between each dimension can be determined by analyzing the moment the triangle is transitioning strips. One critical insight is that the horizontal projection of the brushes must be present on 3 strips when either of the brushes at the corners is about the shift strips. Since the horizontal span of the brushes changes as the brush configuration rotates and the shortest horizontal span occurs when the brush configuration is rotated to position 2 (or position 4) as shown in Figure 5(a), we need to make sure the horizontal span is still sufficient to cover 3 strips. Therefore, a geometric relationship must be satisfied as shown in Equation 3:

$$a \leq H - D - 2b \tag{3}$$

Equation 3 can be used to determine the maximum strip width for maintaining contact with 3 strips during a brush transition; however, issues arise if the strip width is too narrow, such as unintended brush transitions and skipping strips between brushes. Therefore, a minimum strip width is defined which, along with the maximum, establishes a working range for the conductive strip width. The minimum conductive strip width is determined by considering the distance between the central brush and any of the 3 remaining brushes in the geometric configuration, which is the vertex to center distance in the equilateral triangle. The summation of this distance with the brush diameter defines the minimum strip width. This constraint is illustrated by considering the horizontal projection of position 2 (Figure 5(b)) as brush 1 transitions strips, since if the strip width is too narrow, brush 2 will begin transitioning strips prematurely. This relation is quantified in Equation 4, where $L/\sqrt{3}$ is the vertex to center distance:

$$a \geq \frac{L}{\sqrt{3}} + D \tag{4}$$

The final constraint is that the thickness of the brush must be thinner than the width of the insulating strips. If the diameter of the brush is equal or larger than the width of the insulating strip,

a short circuit occurs. It is assumed that all brushes are of equal diameter, and this constraint results in the inequality in Equation 5:

$$b > D \tag{5}$$

2.2.2.5 Determining Geometry Size

The space available under the robot has an area of 6 inch wide by 3.488 inch long. This means that the size to be selected for the geometrical configuration is constrained to this area. To keep the brushes within this area, H (see Figure 6(b)) was chosen to be 2.00 inch. Then from this dimension, the length of the sides of the triangle, L, were calculated to be:

$$L = H\ \frac{2}{\sqrt{3}} \tag{6}$$

$$L = (2.00)\ \frac{2}{\sqrt{3}}$$

$$L = 2.32\ in$$

Increments of 1/32 inch were used to find the brush diameter and the width of the insulating strips. It was decided that since the width of the insulating strips should be larger than the diameter of the brush, the width of the insulating strip should be the next increment of 1/32 inch. These values were introduced in Equations 3 and 4 simultaneously and plotted in Figure 7:

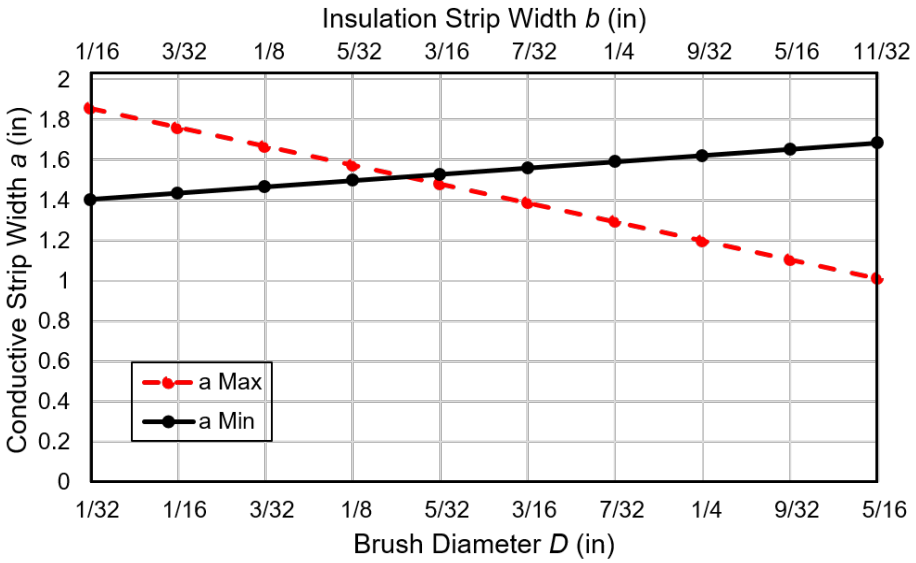

Figure 7. Plot of the conductive strip width as a function of the brush diameter, along with the insulation strip width which corresponds to each brush diameter.

From Figure 7, any combination where $a_{max} > a_{min}$ meets the geometric requirements of the brush design. However, a combination of 1/8 inch and 5/32 inch for the brush diameter and the width of the insulating strips, respectively, were selected for this design, since increments of 1/32 inch are commercially produced. Based on the calculation of the height H, the maximum and minimum size for the conductive strips can then be calculated by Equations 3 and 4, in addition to the brush diameter and insulating strip width determined via Figure 7:

$$a_{max} \leq 1.5725 \tag{7}$$

$$a_{min} \geq 1.46 \tag{8}$$

Therefore, the width of the conductive strips should be between 1.5725 inch and 1.46 inch, and the intermediate value of 1.5 inch was chosen as the final conductive strip width.

2.2.3 Brush Material Selection

Based on our design requirements, the brush needs to be able to carry at least 10 amps of current without causing a drop on the voltage. Assuming the maximum voltage drop allowed on the brush is 0.025 volt (0.2% of 12 volts), the maximum resistance of the brush can be calculated to be 0.0025 Ω. Based on the geometry described in the previous section, the diameter of the brushes was found to be 1/8 inch. Assuming the length of the brush is 1 inch, we can determine the resistivity of the brush material based on Equation 1:

$$\rho = 30\ \mu\Omega\text{-}in \tag{9}$$

Therefore, a copper-tungsten alloy with a composition of 30% copper and 70% tungsten (W70Cu30) was chosen for the brushes, which has a resistivity of 28.34 μΩ-in [25]. In addition, the brushes need to be hard enough to withstand the constant friction forces, without scratching or damaging the floor. It is known that the copper tungsten alloy has a Rockwell Hardness (B) of B85-92 [26] while 304 stainless steel has a hardness of B82 [24]. These properties being similar in magnitude will make it very difficult for the brushes to damage the stainless steel, while still allowing the brushes to be easily machined to the proper length and shape. Other candidate brush materials, such as copper and graphite, were shown to be either be too soft or brittle, or require a much larger brush diameter for this specific application.

2.2.4 Brush Holder Design

Through implementing the established geometry and dimensions, the brush apparatus was designed as shown in Figure 8. The final dimensions of this design are then presented in Figure 9.

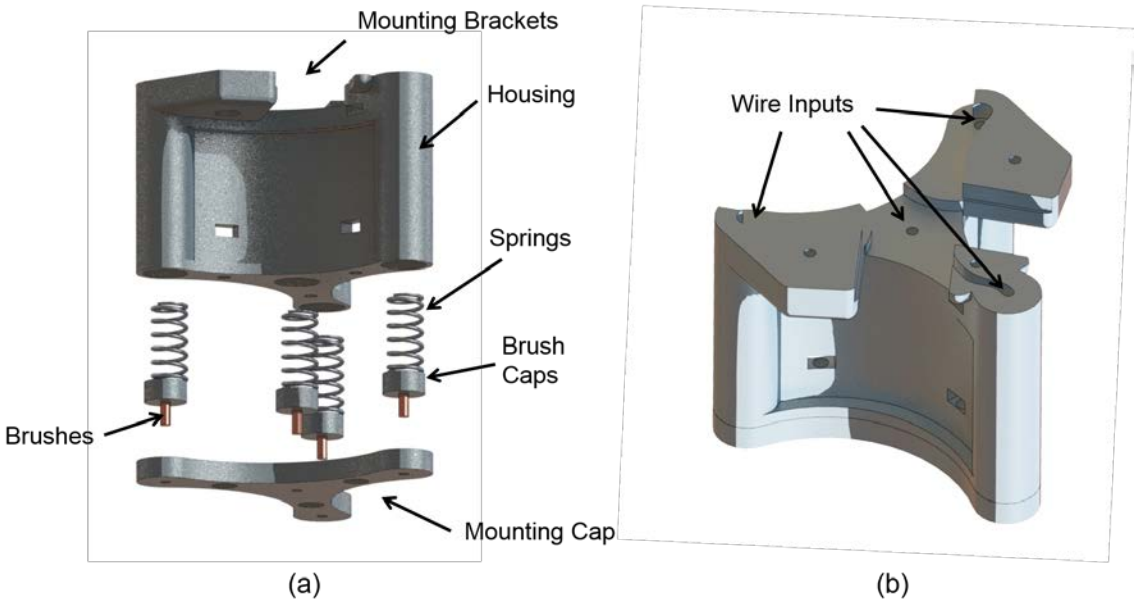

Figure 8. (a) Labeled exploded view of brush holder assembly; (b) brush holder mounting brackets and wire inputs.

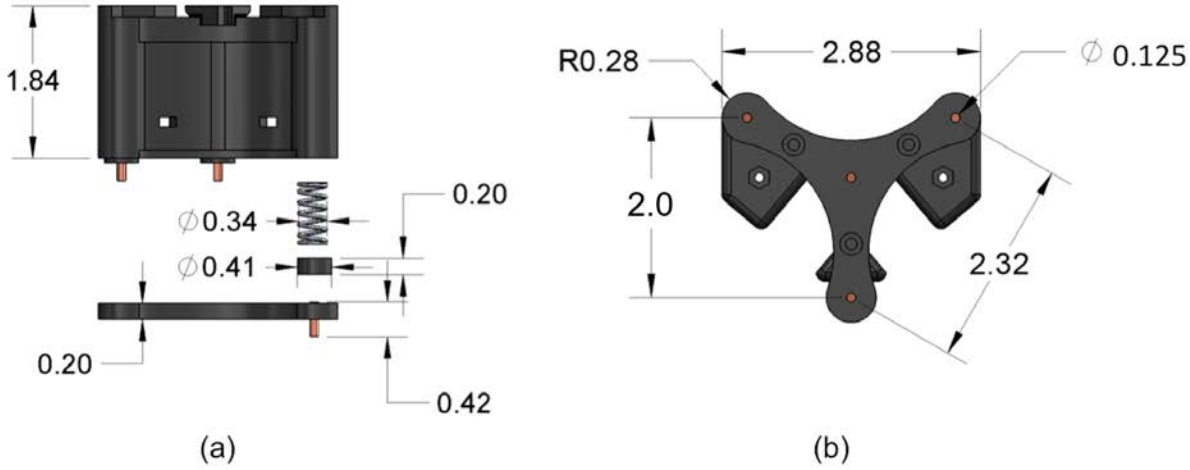

Figure 9. Dimensions of the designed brush apparatus: (a) front view; (b) top view (all units in inches).

To ensure constant connection with the floor despite any debris or defects, springs were mounted between the brushes and the robot. These springs apply a downward force on the brushes into the floor, ensuring a constant connection as the robot moves along the surface. Furthermore, if there is an inconsistency with the surface of the floor, the spring will allow the brush to rise or fall accordingly, and as the brushes wear down over time, more material is extruded as needed. This allows for less frequent maintenance of the robots. The springs must have enough strength to ensure a good connection, but not too strong as to cause unnecessary friction on the brushes.

In order to ease assembly and increase strength, it was decided to mount all four brushes in a single housing that contains all of the components. This housing is rigid and consistent with the previously determined brush geometry. The housing is mounted directly to the underside of the robot using three simple screw and bolt attachment points. The top of the brush holder is designed to fit snugly around the X shaped supports underneath the bot (see Figure 1). This housing descends downwards towards the floor with four vertical hollow tubes that contain the springs and brushes, and allows the components to move freely inside. The housing is then capped off sealing the components inside the tubes, while allowing the brushes to extrude out of the housing and make contact with the floor. This cap is fastened using screws and bolts. The entire housing is suspended one millimeter off the floor, allowing the springs to push out the brushes and fill the difference. A small gap was chosen to reduce the effect of linear and bending forces on the brushes by providing more support.

2.2.4 Cost Analysis

For future manufacturing on a larger scale, the brush material needs to be relatively cheap and easy to obtain. Copper tungsten alloy can be bought easily online and in bulk. The average cost of W70Cu30 tungsten copper alloy is around $17 per square inch, or roughly $8.5 per robot. These prices drop drastically when large quantities are bought in bulk. This is a good price for the application and quality of the material.

2.3 Rectifier Circuit

2.3.1 Design Constraints

As the mobile 3D printer moves across the floor surface, the alternating polarity received through the brushes must be sorted such that current flows in the correct direction for use onboard the printer. A rectifier circuit was developed to accomplish this goal, and was subject to the following design constraints:

1. Dynamic brushes: To keep cost and size to a minimum, a single brush must be able to switch from positive and negative current depending on its location. That is, the onboard rectifier circuit must separate and organize the charge no matter which brush it is coming from. For example, as long as one brush is positive and one brush is negative, the circuit forces the current to flow in the correct direction through the robot. This allows for a single brush to accept both positive and negative currents without causing a short circuit, thereby reducing the total number of brushes required.
2. Power: The circuit needs to be able to handle the supplied voltage of 12 volts and 10 amps safely and without overheating.
3. Four brush sorting: The circuit must sort the current of all four brushes simultaneously.
4. Volumetric constraints: The entire circuit must be small enough to fit onto the robot without interfering with the existing electronics and mechanical systems.

2.3.2 Circuit Design

The rectifier circuit design shown in Figure 10 was created according to the specified engineering requirements. Each brush is connected to two Schottky diodes, in forward and reversed bias, making a total of 8 Schottky diodes in the rectifier circuit. Every time a brush is connected to a conductive strip, one of the diodes will be closed and the other will be open. This mechanism allows the current to always flow in the same direction through the rectifier circuit. In addition, there is an electrolytic capacitor connected in parallel to one of the ends of each of the diodes. The electrolytic capacitor has the functionality of storing small amounts of charges during operation, thereby avoiding electric sparks when passing from one strip to the other. This minimizes the risk of fires or electrocution.

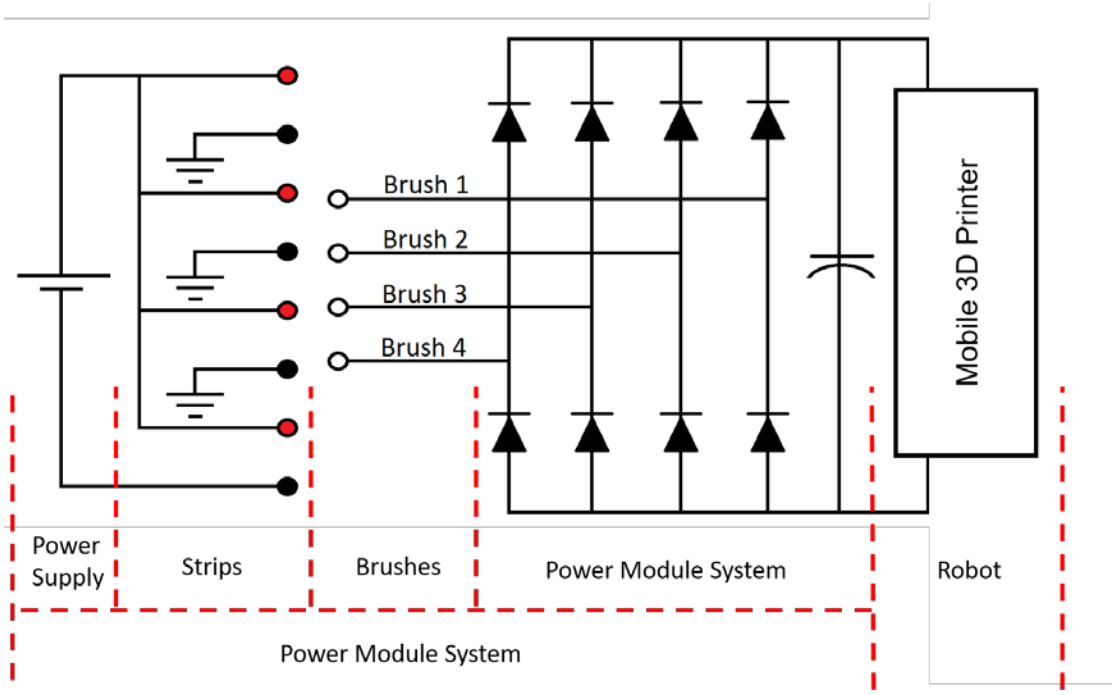

Figure 10. Circuit diagram of the complete system, where each component is labeled by region.

3. Prototyping

3.1 Floor Surface

3.1.1 Prototyping Considerations

A cement base was chosen because it would be non-conductive, is readily available, and would not deform under stress. In the future, the base could be any rigid non-conducting surface or floor. The cement was poured into a 2 x 2 ft. mold until approximately 1 inch thick, with carbon fiber rebar inserted for additional strength and crack prevention. Although the floor would not likely be experiencing wide temperature changes or tensile stresses, rebar was necessary so that no catastrophic damage occurred during transportation. Using cement demonstrated the viability of implementing this design on a large-scale factory floor.

3.1.2 Fabrication Process

A 14 V power supply was used at this stage to prevent the possibility of a voltage drop across the prototype floor surface interfering with the performance of the mobile 3D printer, which requires a 12 V operation voltage. The floor surface was then fabricated using cement, 304 stainless steel strips, and marine grade epoxy through the following steps (corresponding to the steps depicted in Figure 11):

Step 1: Cement was poured into a mold with a flat bottom until it is halfway full. This becomes the base of the floor surface. Carbon fiber rebar was placed on top of the cement.

Step 2: The rest of the mold was filled with concrete. Once dried the concrete base was removed from the wooden mold.

Step 3: It is necessary that the spacing between strips is uniform across the floor. Two plastic spacers were designed and printed to fit over the ends of the strips while they were on the cement base. The spacers would maintain the gap between adjacent strips while the strips were adhered together using duct tape.

Step 4: The strips were then removed from the cement base so that a very thin layer of marine epoxy can be spread over the surface. It is necessary to minimize the amount of epoxy used, as excess would result in humps and dips on the final floor surface. With the epoxy applied, the strips were placed back on the surface, and several weights were put on top to ensure even contact between the strips and the epoxy. The epoxy was left to cure for 24 hours.

Step 5: Once the strips were fully adhered to the cement, epoxy was applied to the gaps between the metal strips. These would serve as the insulating strips on the floor surface. After the epoxy had cured, it was sanded down so the surface was flat. At this point, areas where the epoxy had not filled in the gaps, or where bubbles had formed were identified, and additional epoxy was applied and allowed to cure.

Step 6: Each strip was then connected to a 14 V power supply, with each strip alternating positive and negative. Finally, the finished floor was housed in a recessed box to prevent inadvertent contact by users and to allow discrete mounting of the power supply. The final floor assembly was sanded down a final time, which yielded a flat surface.

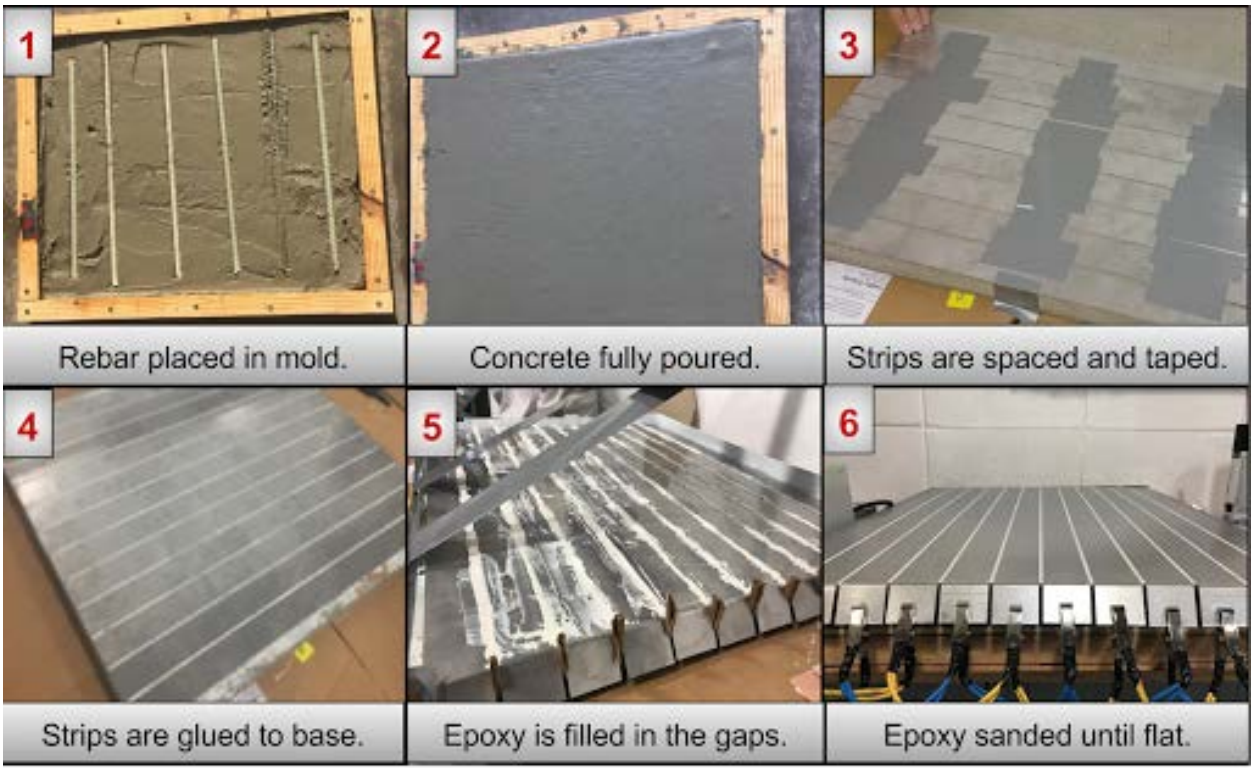

Figure 11. Floor prototype construction process.

3.2 Brush Apparatus

3.2.1 Fabrication Process

With the fundamental design established, prototyping began with 3D printing the brush housing with an uPrint SE Plus 3D printer. 3D printing was the best option for prototyping, since it allows for prototypes to be made quickly and cheaply, and thus makes it possible to have many iterations early in the design process. The fabrication process followed was:

Step 1: The copper-tungsten brushes (Figure 8(a)) were machined from a single 1/8 in diameter rod. First, the rod was cut by hand into 4 equal brushes of 0.5 in long. Then, the end that makes contact with the floor was machined to be smooth, and a small bevel was added to the edge to remove any sharp edges prone to snagging.

Step 2: To wire the brushes, a small hole was drilled into the face of each brush facing the housing (Figure 8(a)), and wires were tapped into these holes and secured with superglue (cyanoacrylate).

Step 3: The brush caps were then installed around each brush, which increases stability and provides a platform on which each spring makes a solid connection.

Step 4: The springs and brushes were loaded into the housing (Figure 8(a)). The wire was fed through the hollow tubes, through the center of the spring, and out through the wire outputs labeled in Figure 8(b).

Step 5: The entire assembly was locked together by first attaching the housing cap to the main housing with screws. Then, the complete brush apparatus was mounted to the base of the robot, as seen in Figure 12.

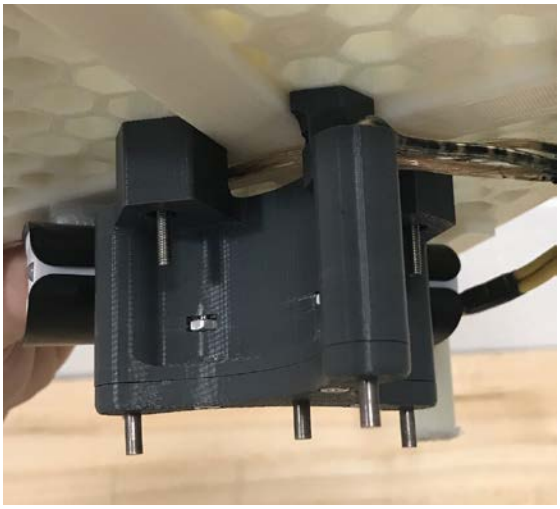

Figure 12. Prototype of brush apparatus.

3.3 Rectifier Circuit

3.3.1 Component Selection

The rectifier circuit is composed of a total of 8 Schottky diodes mounted on a printed circuit board (PCB) and arranged as is shown in Figure 13. The Schottky diodes were selected because of their great capability to withstand high frequency of change of polarities. A 1000 μF electrolytic capacitor was connected in parallel to each brush, as is shown in Figure 10. The PCB selected for the rectifier circuit is a 2 layer PCB with an area of 63.6 mm by 51.3 mm and a thickness of 1.02 mm. This double layer PCB has one layer of copper and other one of an insulating material.

3.3.2 Fabrication Process

The layout of the circuit board was CNC machined and is shown in Figure 13. The steps of assembling the rectifier circuit are as follows:

Step 1: The eight Schottky diodes, the 1000 μF electrolytic capacitor, the terminals of the four brushes, and the terminals of the positive and negative poles that feed to the 3D printer circuit are each mounted on the PCB in the orientation shown in Figure 9.

Step 2: All electronic components were soldered by hand. Because of this, the spacing between the components was left wide enough to easily solder the components, and to allow sufficient room for the components to cool off during operation. Further studies will be carried out to determine the optimal spacing for the components to cool off or if additional heat sinks will be needed, and later models will be soldered automatically in a circuit printing machine.

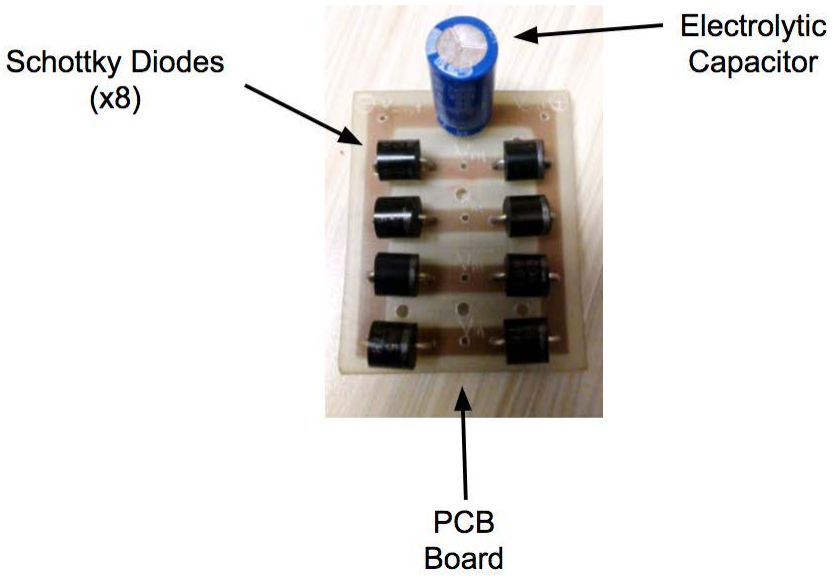

Figure 13. Rectifier circuit prototype.

4. Results

4.1 Preliminary Testing

The floor power module was first tested by measuring if the conductive strips were consistently providing the necessary voltage. With the power supply connected to each strip alternating positive and negative, ideal performance would entail 14 V being read at any point across 2 opposite polarity strips. After the power supply was powered on, a voltmeter was used to test the voltage between strips. This measured a voltage of ~14.1 V at any point along the floor surface, verifying that the prototype was functional. This testing process may be seen in Figure 14:

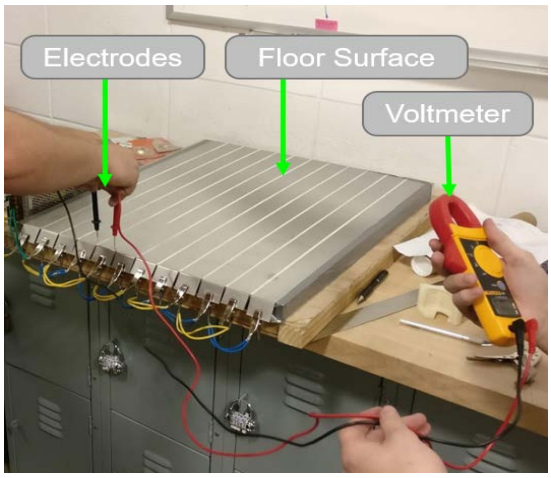

Figure 14. Strip voltage test setup.

Next, a test was performed to show that the brushes could adequately and safely transfer the power from the floor to the mobile robot. A mock robot was constructed to test the floor power module prior to testing the mobile 3D printer to protect the real robot from any potential dangers. This mock robot is a replica of the real robot minus any hardware not necessary for testing the function of the brushes and circuit. The mock robot is shown in Figure 15. The mock robot is built upon an identical base to that of the mobile 3D printer, and contains all components of the floor power module. In addition, it contains a dummy load which simulates the resistance of the 3D printer in operation. This allows all components to be mounted in their intended arrangement.

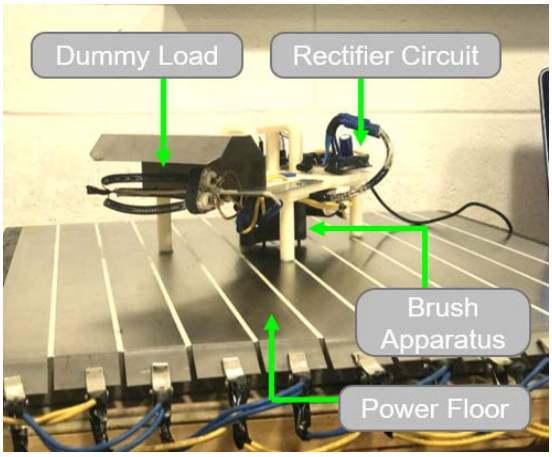

Figure 15. Mock robot on floor surface.

For mock robot testing, the prototype for the brush apparatus was mounted to an identical base for the robot that will be used. Then, the brushes were connected to an Arduino equipped with a voltage and amperage meter in order to record and display the results. The floor was then fully powered and the mock robot with brushes equipped was moved around the floor by hand, accounting for every possible angle and position. Also, the mock robot was quickly lifted off of the floor to demonstrate what would happen in an unwanted case of disconnection. The results and corresponding path of movement can be seen in Figure 16:

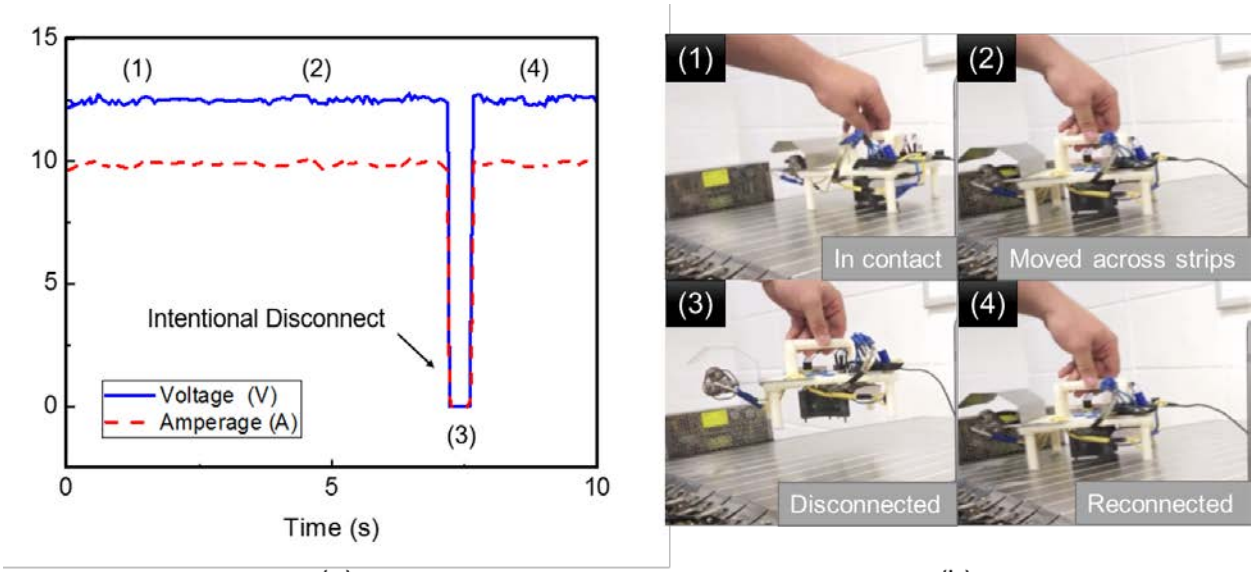

Figure 16. Mock robot test of floor power module: (a) current and voltage against time; (b) path of movement for mock robot during test.

As desired, the robot received a constant 12 V and 10 A without any dangerous spikes or drops. When the robot becomes disconnected the power immediately drops to 0 W, and when connected it immediately regains full power. These are the results that were desired and designed for.

4.2 Testing with Mobile 3D Printer

Once confident in the safety of the floor and brushes, testing was continued with the real robot. The brush apparatus was mounted to the robot and wired to its onboard microcontroller. The robot was then placed on the floor surface and power was switched on, the robot immediately powered up. A G-code script was uploaded to the robot to perform a simple rectangular path along the floor to test connection and power. The robot ran without any interruptions, and this test can be seen in Figure 17. Other paths have been uploaded to the robot and they have been performed successfully as well. The results show the promise for a full implementation of this design in large scale in a factory setting.

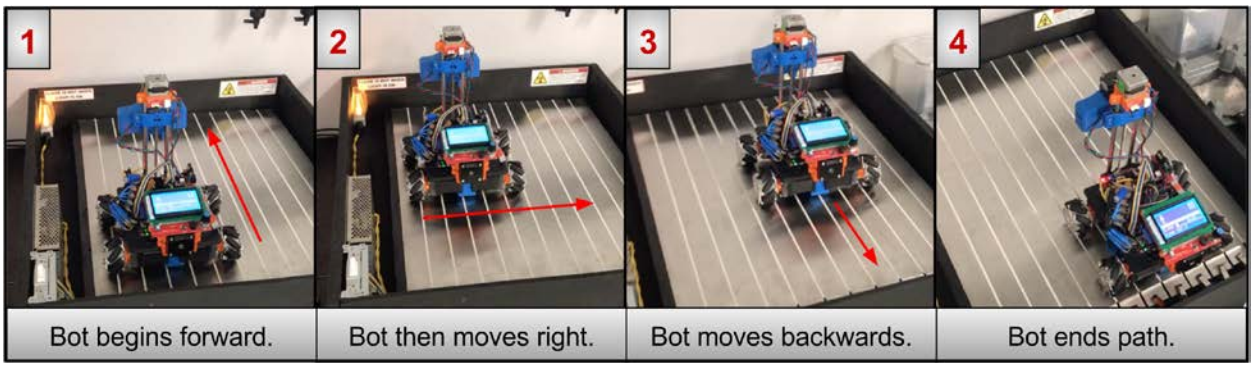

Figure 17. Robot moving across the floor power module, without any additional power sources. Each image follows chronologically from the previous.

5. Conclusions

This paper presented a scalable floor power module to wirelessly power mobile 3D printers for a cooperative 3D printing platform. First, design requirements and constraints were established for each component. These requirements and restrictions guided the overall design to emulate bumper car powering technology, and it was established that a powered floor, brush apparatus onboard the printer, and a rectifier circuit must each be designed to achieve the goal of wirelessly powering mobile 3D printers. These components were then prototyped and tested by measuring the potential difference across the floor surface, followed by running a mock robot equipped with each component. Testing results showed that the mobile 3D printers can successfully be powered wirelessly by a conducting floor power module and a brush apparatus mounted beneath the robot. The intended impact of this design is to expand the overall printing envelope of 3D printing and to enable cooperative printing through the use of mobile printers by providing constant untethered power. By enabling cooperative 3D printing on a large scale, the technology of 3D printing advances towards being a competitive digital manufacturing method.

6. Acknowledgements

We gratefully acknowledge the financial support from the University of Arkansas, through the startup fund provided by the Vice Provost Office for Research and Economic Development. Any opinions, findings, and conclusions or recommendations expressed in this publication are those of the authors and do not necessarily reflect the views of the University of Arkansas.

7. References

[1] Billiet, T., Vandenhaute, M., Schelfhout, J., 2012, "A Review of Trends and Limitations in Hydrogel-Rapid Prototyping for Tissue Engineering," Biomaterials, 33(26) pp. 6020-6041.
[2] Campbell, I., Bourell, D., and Gibson, I., 2012, "Additive Manufacturing: Rapid Prototyping Comes of Age," Rapid Prototyping Journal, 18(4) pp. 255-258.
[3] Macdonald, E., Salas, R., Espalin, D., 2014, "3D Printing for the Rapid Prototyping of Structural Electronics," IEEE Access, 2pp. 234-242.
[4] Weller, C., Kleer, R., and Piller, F., 2015, "Economic Implications of 3D Printing: Market Structure Models in Light of Additive Manufacturing Revisited," International Journal of Production Economics, 164pp. 43-56.
[5] Oropallo, W., and Piegl, L., 2016, "Ten Challenges in 3D Printing," Engineering with Computers, 32(1) pp. 135-148.
[6] Gao, W., Zhang, Y., Ramanujan, D., 2015, "The Status, Challenges, and Future of Additive Manufacturing in Engineering," Computer-Aided Design, 69pp. 65-89.
[7] R. C. Luo, C. H. Huang, and C. Y. Huang, 2010, "Search and track power charge docking station based on sound source for autonomous mobile robot applications," 2010 IEEE/RSJ International Conference on Intelligent Robots and Systems, Anonymous pp. 1347-1352.
[8] Wattanasin, C., Aiyama, Y., Kurabayashi, D., 2001, "Hybrid Power Supply for Mobile Robots," Advanced Robotics, 15(6) pp. 695-710.

[9] Wu, J., Qiao, G., Ge, J., 2012, "Automatic Battery Swap System for Home Robots," International Journal of Advanced Robotic Systems, 9(6) pp. 255.
[10] Youn-Ho Choi, and Dong-Ha Lee, 2013, "Battery swap station for mobile robot," 2013 International Conference on Electrical Machines and Systems (ICEMS), Anonymous pp. 1445-1447.
[11] J. B. Siegel, Y. Wang, A. G. Stefanopoulou, 2015, "Comparison of SOFC and PEM Fuel Cell Hybrid Power Management Strategies for Mobile Robots," 2015 IEEE Vehicle Power and Propulsion Conference (VPPC), Anonymous pp. 1-6.
[12] Logan, D., Pentzer, J., Brennan, S., 2012, "Comparing Batteries to Generators as Power Sources for use with Mobile Robotics," Journal of Power Sources, 212pp. 130-138.
[13] M. M. Sadeghi, and E. F. Kececi, 2016, "Hybrid power system for mobile robotics," 2016 International Conference on System Reliability and Science (ICSRS), Anonymous pp. 64-67.
[14] A. Sulaiman, F. Inambao, and G. Bright, 2013, "Development of solar hydrogen energy for mobile robots," 2013 6th Robotics and Mechatronics Conference (RobMech), Anonymous pp. 14-19.
[15] Amundson, K., Raade, J., Harding, N., 2006, "Development of Hybrid Hydraulic-Electric Power Units for Field and Service Robots," Advanced Robotics, 20(9) pp. 1015-1034.
[16] Raade, J. W., and Kazerooni, H., 2005, "Analysis and Design of a Novel Hydraulic Power Source for Mobile Robots," IEEE Transactions on Automation Science and Engineering, 2(3) pp. 226-232.
[17] Riofrio, J. A., and Barth, E. J., 2007, "A Free Piston Compressor as a Pneumatic Mobile Robot Power Supply: Design, Characterization and Experimental Operation," International Journal of Fluid Power, 8(1) pp. 17-28.
[18] Sulaiman, A., Inambao, F., and Bright, G., 2014, "Solar-Hydrogen Energy as an Alternative Energy Source for Mobile Robots and the New-Age Car," IOP Conference Series: Materials Science and Engineering, 65.
[19] Wilhelm, A. N., Surgenor, B. W., and Pharoah, J. G., 2006, "Design and Evaluation of a Micro-Fuel-Cell-Based Power System for a Mobile Robot," IEEE/ASME Transactions on Mechatronics, 11(4) pp. 471-476.
[20] A. Mandow, J. M. Gomez-de-Gabriel, J. L. Martinez, 1996, "The Autonomous Mobile Robot AURORA for Greenhouse Operation," IEEE Robotics & Automation Magazine, 3(4) pp. 18-28.
[21] D'Andrea, R., 2012, "A Revolution in the Warehouse: A Retrospective on Kiva Systems and the Grand Challenges Ahead," Ieee Transactions on Automation Science and Engineering, 9(4) pp. 638-639.
[22] Eyerly, Jon V. Bumper Car Amusement Ride. Eyerly Jon V, assignee. Patent US 4324301 A. 28 Feb. 1980. Print.
[23] Collaboration of NDT Education, 2002, "Conductivity and Resistivity Values for Iron & Alloys," **2017**(04/12) .
[24] AK Steel Corporation, 2007, "304/304L Stainless Steel; UNS S30400/UNS S30403," **2017**(04/15) .
[25] Torrey Hills Technologies, L., "Copper Tungsten Technical Data," **2017**(04/15) .
[26] WHS Sondermetalle, 2014, "Data Sheet: Tungsten-Copper (WCu)," **2017**(04/15) .